

Research topics on flow-induced vibrations

PEF 6000 - Special topics on dynamics of structures

Associate Professor Guilherme R. Franzini

- 1 Objectives
- 2 Vortex-induced vibrations (VIV)
- 3 Passive suppression of galloping
- 4 Vortex-self induced vibrations (VSIV)
- 5 Energy harvesting

- To present research topics on flow-induced vibrations;

- To present research topics on flow-induced vibrations;
- To highlight the contributions from EPUSP to the state-of-art.

- To present research topics on flow-induced vibrations;
- To highlight the contributions from EPUSP to the state-of-art.
- References: MsC dissertation written by Tatiana Ueno (2019), habilitation thesis written by Gonçalves (2013, Fajarra (2013), Rateiro (2014) and Franzini (2019) and selected papers.

VIV still demands some investigations. Examples of open topics include:

- Flow around cylinders with low aspect ratio;

VIV still demands some investigations. Examples of open topics include:

- Flow around cylinders with low aspect ratio;
- Flow around cylinders with cross-sections other than circular;

VIV still demands some investigations. Examples of open topics include:

- Flow around cylinders with low aspect ratio;
- Flow around cylinders with cross-sections other than circular;
- Passive control;

VIV still demands some investigations. Examples of open topics include:

- Flow around cylinders with low aspect ratio;
- Flow around cylinders with cross-sections other than circular;
- Passive control;
- Flexible cylinder VIV;

VIV still demands some investigations. Examples of open topics include:

- Flow around cylinders with low aspect ratio;
- Flow around cylinders with cross-sections other than circular;
- Passive control;
- Flexible cylinder VIV;
- Concomitant excitation.

- Monocolumn platforms have low aspect ratio ($L/D < 5$);

- Monocolumn platforms have low aspect ratio ($L/D < 5$);
- The flow around these structures lead to oscillatory responses on the horizontal plane with amplitudes of order of one diameter (Vortex-Induced Motion - VIM);

Flow around cylinders with low aspect ratio

- Monocolumn platforms have low aspect ratio ($L/D < 5$);
- The flow around these structures lead to oscillatory responses on the horizontal plane with amplitudes of order of one diameter (Vortex-Induced Motion - VIM);
- Tridimensional effects are of great importance (other flow structures than the von Kármán wake);

Flow around cylinders with low aspect ratio

- Monocolumn platforms have low aspect ratio ($L/D < 5$);
- The flow around these structures lead to oscillatory responses on the horizontal plane with amplitudes of order of one diameter (Vortex-Induced Motion - VIM);
- Tridimensional effects are of great importance (other flow structures than the von Kármán wake);
- Lower branch is not so well defined;

- Monocolumn platforms have low aspect ratio ($L/D < 5$);
- The flow around these structures lead to oscillatory responses on the horizontal plane with amplitudes of order of one diameter (Vortex-Induced Motion - VIM);
- Tridimensional effects are of great importance (other flow structures than the von Kármán wake);
- Lower branch is not so well defined;
- Examples of references: Gonçalves (2013), Fugarra (2013), Gonçalves et al (2015)...

- Floating platforms may exhibit cross-sections different from the circular one;

- Floating platforms may exhibit cross-sections different from the circular one;
- Examples of usual cross-sections: Square sections, with rounded corners;

- Floating platforms may exhibit cross-sections different from the circular one;
- Examples of usual cross-sections: Square sections, with rounded corners;
- Possible coexistence of galloping and VIV;

- Floating platforms may exhibit cross-sections different from the circular one;
- Examples of usual cross-sections: Square sections, with rounded corners;
- Possible coexistence of galloping and VIV;
- Gonçalves et al (2015): Oscillation amplitude strongly depends of the angle of attack;

- Floating platforms may exhibit cross-sections different from the circular one;
- Examples of usual cross-sections: Square sections, with rounded corners;
- Possible coexistence of galloping and VIV;
- Gonçalves et al (2015): Oscillation amplitude strongly depends of the angle of attack;
- Gonçalves et al (2016): Experimental investigation on the effects of round corners.

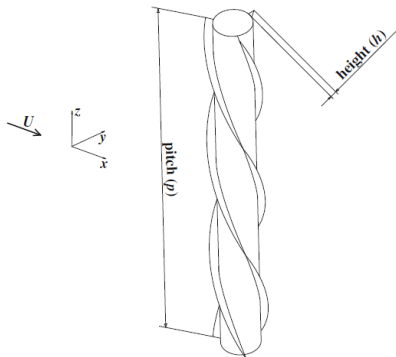


Figura: Extraído de Korkischko & Meneghini (2011).

- The flow separation occurs at fixed points located at the *strakes*;

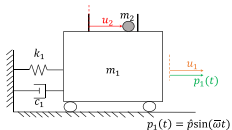
- The flow separation occurs at fixed points located at the *strakes*;
- Decreases the correlation length;

Passive suppression - *strakes*

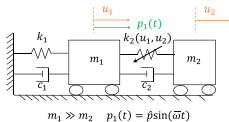
- The flow separation occurs at fixed points located at the *strakes*;
- Decreases the correlation length;
- Direct interference on the flow field.

Passive suppression - NVA

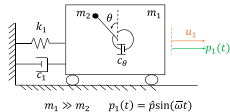
- NVA (Nonlinear vibration absorber) or NES (Nonlinear Energy Sink): Mass coupled to the main structure by means of an element of null linearized natural frequency and a dashpot. Examples of NVA are (from Franzini (2019));



(a) VI-NES.



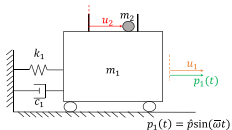
(b) Translative NVA.



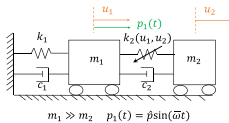
(c) Rotative NVA.

Passive suppression - NVA

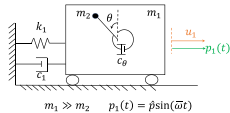
- NVA (Nonlinear vibration absorber) or NES (Nonlinear Energy Sink): Mass coupled to the main structure by means of an element of null linearized natural frequency and a dashpot. Examples of NVA are (from Franzini (2019));



(a) VI-NES.



(b) Translative NVA.

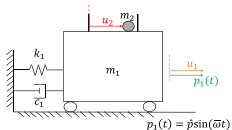


(c) Rotative NVA.

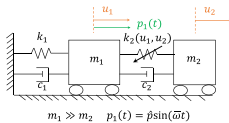
- No preferential frequency for suppression;

Passive suppression - NVA

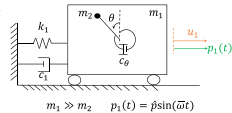
- NVA (Nonlinear vibration absorber) or NES (Nonlinear Energy Sink): Mass coupled to the main structure by means of an element of null linearized natural frequency and a dashpot. Examples of NVA are (from Franzini (2019));



(a) VI-NES.



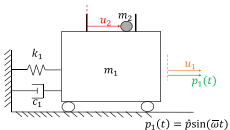
(b) Translative NVA.



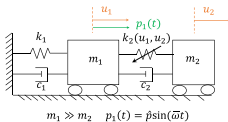
(c) Rotative NVA.

- No preferential frequency for suppression;
- Numerical studies based on CFD presented in Tumkur et al (2013a,b) and Blanchard (2016): A rotative NVA is efficient in VIV mitigation;

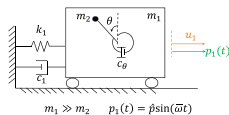
- NVA (Nonlinear vibration absorber) or NES (Nonlinear Energy Sink): Mass coupled to the main structure by means of an element of null linearized natural frequency and a dashpot. Examples of NVA are (from Franzini (2019));



(a) VI-NES.



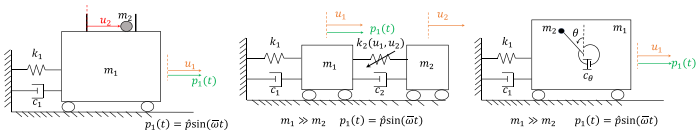
(b) Translative NVA.



(c) Rotative NVA.

- No preferential frequency for suppression;
- Numerical studies based on CFD presented in Tumkur et al (2013a,b) and Blanchard (2016): A rotative NVA is efficient in VIV mitigation;
- CFD calculations have high computational cost → Sensitivity studies with respect to changes in the NVA parameters are practically impossible;

- NVA (Nonlinear vibration absorber) or NES (Nonlinear Energy Sink): Mass coupled to the main structure by means of an element of null linearized natural frequency and a dashpot. Examples of NVA are (from Franzini (2019));



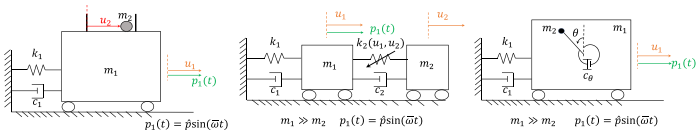
(a) VI-NES.

(b) Translative NVA.

(c) Rotative NVA.

- No preferential frequency for suppression;
- Numerical studies based on CFD presented in Tumkur et al (2013a,b) and Blanchard (2016): A rotative NVA is efficient in VIV mitigation;
- CFD calculations have high computational cost → Sensitivity studies with respect to changes in the NVA parameters are practically impossible;
- On the other hand, wake-oscillators appear as an interesting alternative;

- NVA (Nonlinear vibration absorber) or NES (Nonlinear Energy Sink): Mass coupled to the main structure by means of an element of null linearized natural frequency and a dashpot. Examples of NVA are (from Franzini (2019));



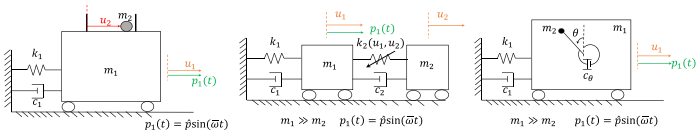
(a) VI-NES.

(b) Translative NVA.

(c) Rotative NVA.

- No preferential frequency for suppression;
- Numerical studies based on CFD presented in Tumkur et al (2013a,b) and Blanchard (2016): A rotative NVA is efficient in VIV mitigation;
- CFD calculations have high computational cost \rightarrow Sensitivity studies with respect to changes in the NVA parameters are practically impossible;
- On the other hand, wake-oscillators appear as an interesting alternative;
- The use of a rotative NVA is focus of the MsC. dissertation written by Ueno (2019) and the paper Ueno & Franzini (2019).

- NVA (Nonlinear vibration absorber) or NES (Nonlinear Energy Sink): Mass coupled to the main structure by means of an element of null linearized natural frequency and a dashpot. Examples of NVA are (from Franzini (2019));



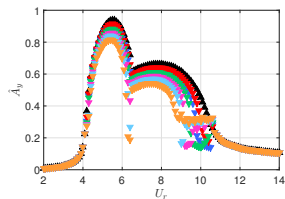
(a) VI-NES.

(b) Translative NVA.

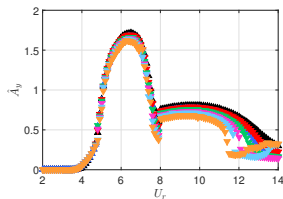
(c) Rotative NVA.

- No preferential frequency for suppression;
- Numerical studies based on CFD presented in Tumkur et al (2013a,b) and Blanchard (2016): A rotative NVA is efficient in VIV mitigation;
- CFD calculations have high computational cost → Sensitivity studies with respect to changes in the NVA parameters are practically impossible;
- On the other hand, wake-oscillators appear as an interesting alternative;
- The use of a rotative NVA is focus of the MsC. dissertation written by Ueno (2019) and the paper Ueno & Franzini (2019).
- At least to the best of the authors' knowledge, passive suppression of VIV-2dof using a rotative NVA was not found in the literature.

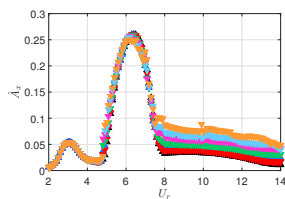
- Results from Ueno (2019) and Ueno & Franzini (2019).
- Use of wake-oscillators allowed developing sensitivity studies with respect to the influence of the NVA on the suppression;
- In the following results: $\hat{r} = 0.50$ e $\zeta_{\theta} = 0.10$. G1-Sim1: $\hat{m} = 0.03$, G1-Sim2: $\hat{m} = 0.07$, G1-Sim3: $\hat{m} = 0.10$, G1-Sim4: $\hat{m} = 0.12$ and G1-Sim5: $\hat{m} = 0.15$.



(a) $\hat{A}_y(U_r)$. VIV-1dof.



(b) $\hat{A}_y(U_r)$. VIV-2dof.

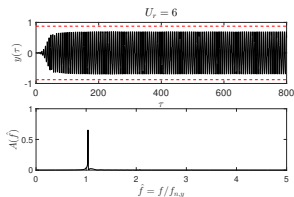


(c) $\hat{A}_x(U_r)$. VIV-2dof.

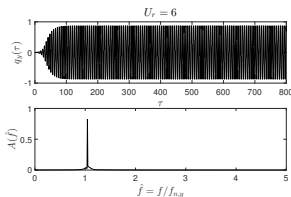
Extracted from Ueno (2019).

Passive suppression - Rotative NVA

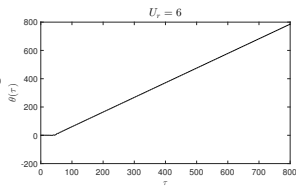
- Example of time-histories $\hat{r} = 0.50$, $\zeta_\theta = 0.10$, $\hat{m} = 0.15$ - $U_r = 6$. VIV-1dof.



(a) $y(\tau)$ and amplitude spectrum.



(b) $q_y(\tau)$ and amplitude spectrum.

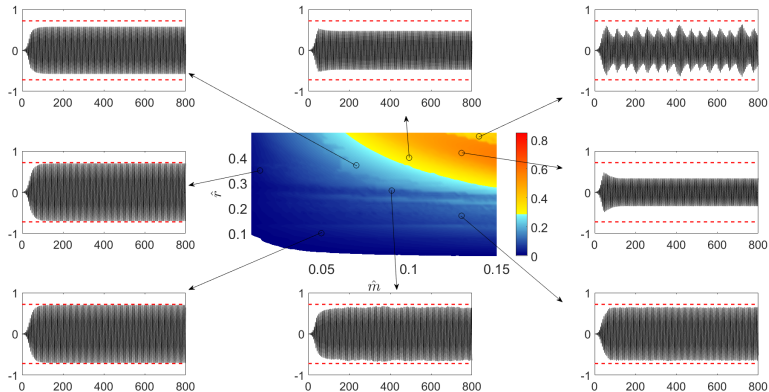


(c) $\theta(\tau)$.

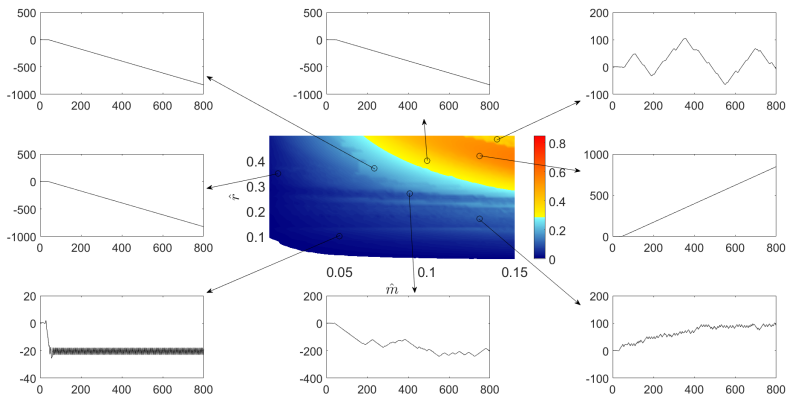
- 1 : 1 : 1 resonance (TET mechanism).

Adapted from Ueno (2019).

- In the colorbar, the map above shows an efficiency criterion. Values close to 1 refer to high efficiency.



Extracted from Ueno (2019).



Extracted from Ueno (2019).

- Already discussed: The response to VIV is intrinsically more intricate than that observed in rigid and elastically supported cylinders;

Flexible cylinders under VIV

- Already discussed: The response to VIV is intrinsically more intricate than that observed in rigid and elastically supported cylinders;
- Derivation of reduced-order models (ROMs): How can we choose a set of projection functions to be adopted in the Galerkin's method?

- Already discussed: The response to VIV is intrinsically more intricate than that observed in rigid and elastically supported cylinders;
- Derivation of reduced-order models (ROMs): How can we choose a set of projection functions to be adopted in the Galerkin's method?
- Possible alternative: “Quasi-Bessel” modes.

Flexible cylinders under VIV

- Already discussed: The response to VIV is intrinsically more intricate than that observed in rigid and elastically supported cylinders;
- Derivation of reduced-order models (ROMs): How can we choose a set of projection functions to be adopted in the Galerkin's method?
- Possible alternative: “Quasi-Bessel” modes.
- Due to the non-linear character of the mathematical model, the system of ODEs will be coupled **How to evaluate the number of adopted modes?**

- Use of wake-oscillators: Forces due to the fluid-structure interaction are distributed along the span;

- Use of wake-oscillators: Forces due to the fluid-structure interaction are distributed along the span;
- Spatial distribution: Nodal (via FEM) continuously?

Flexible cylinders under VIV

- Use of wake-oscillators: Forces due to the fluid-structure interaction are distributed along the span;
- Spatial distribution: Nodal (via FEM) continuously?
- What is the projection function to be adopted in the Galerkin's method for discretizing the PDE associated with the van der Pol equation?

Flexible cylinders under VIV

- Use of wake-oscillators: Forces due to the fluid-structure interaction are distributed along the span;
- Spatial distribution: Nodal (via FEM) continuously?
- What is the projection function to be adopted in the Galerkin's method for discretizing the PDE associated with the van der Pol equation?
- Use of wake-oscillators for flexible cylinder VIV: Is valid to use the empirically calibrated parameters obtained from experiments with rigid and elastically mounted cylinders?

Flexible cylinders under VIV

- Use of wake-oscillators: Forces due to the fluid-structure interaction are distributed along the span;
- Spatial distribution: Nodal (via FEM) continuously?
- What is the projection function to be adopted in the Galerkin's method for discretizing the PDE associated with the van der Pol equation?
- Use of wake-oscillators for flexible cylinder VIV: Is valid to use the empirically calibrated parameters obtained from experiments with rigid and elastically mounted cylinders?
- What is the gain allowed by the use of "non-standard" techniques such as the use of invariant manifolds in VIV analysis?

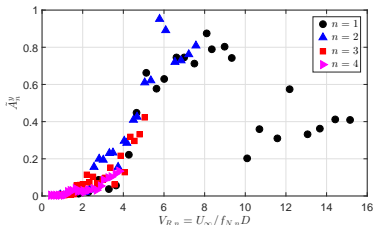
Flexible cylinders under VIV

- Use of wake-oscillators: Forces due to the fluid-structure interaction are distributed along the span;
- Spatial distribution: Nodal (via FEM) continuously?
- What is the projection function to be adopted in the Galerkin's method for discretizing the PDE associated with the van der Pol equation?
- Use of wake-oscillators for flexible cylinder VIV: Is valid to use the empirically calibrated parameters obtained from experiments with rigid and elastically mounted cylinders?
- What is the gain allowed by the use of “non-standard” techniques such as the use of invariant manifolds in VIV analysis?
- A comprehensive research project on nonlinear dynamics of risers was developed at EPUSP and LMO led the experimental activities. This class brings experimental results from this project.

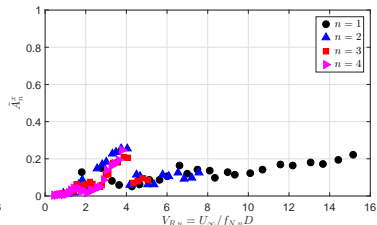
- Modal decomposition: Decompose the measured data into a set of projection functions. **Allows identifying the participation of different modes in the response.**

$$\tilde{a}_n^x(t_j) = \frac{\int_0^1 X^*(z, t_j) \psi_n(z) d\xi}{\int_0^1 (\psi_n(z))^2 d\xi} \quad (1)$$

$$\tilde{a}_n^y(t_j) = \frac{\int_0^1 Y^*(z, t_j) \psi_n(z) d\xi}{\int_0^1 (\psi_n(z))^2 d\xi} \quad (2)$$



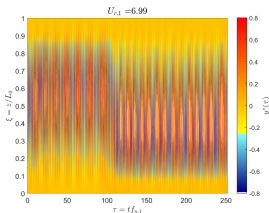
(a) Cross-wise characteristic modal-amplitude oscillation \tilde{A}_n^y .



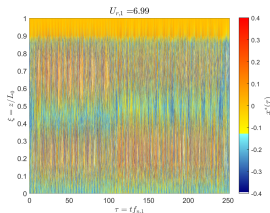
(b) In-line characteristic modal-amplitude oscillation \tilde{A}_n^x .

Extracted from Franzini et al (2016).

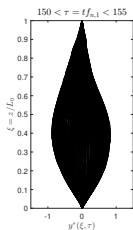
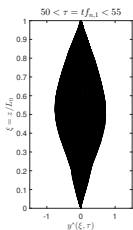
Different regimes may appear in the same nominal modal reduced velocity $U_{r,1} = U_{\infty}/f_{n,1}D$. The figure below is extracted from Franzini (2019).



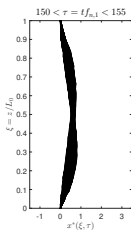
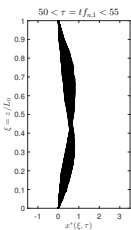
(a) Scalogram $y^*(\xi, \tau)$.



(b) Scalogram $x^*(\xi, \tau)$.

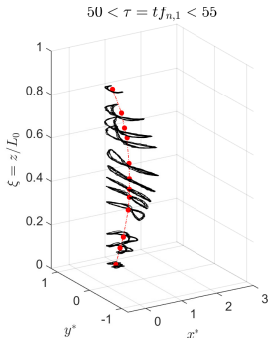


(c) Instantaneous deformed cross-wise configuration.

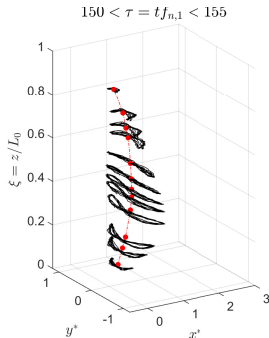


(d) Instantaneous deformed in-line configuration.

Trajectories on the horizontal plane.



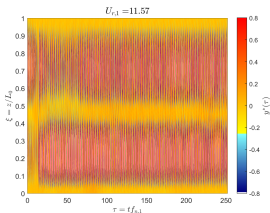
(a) $50 < \tau < 55$.



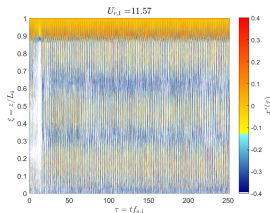
(b) $150 < \tau < 155$.

Extracted from Franzini (2019).

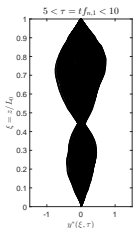
The figure below is extracted from Franzini (2019).



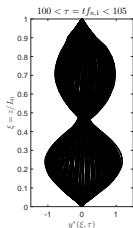
(a) Scalogram $y^*(\xi, \tau)$.



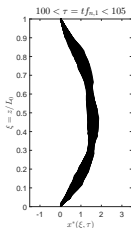
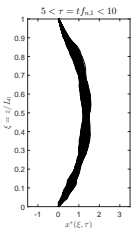
(b) Scalogram $x^*(\xi, \tau)$.



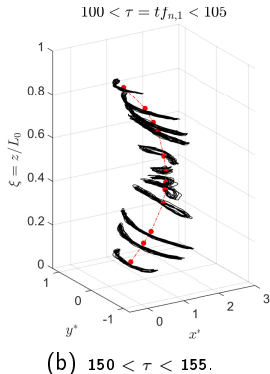
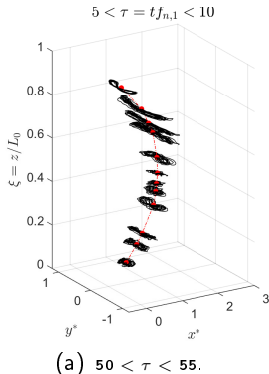
(c) Instantaneous deformed cross-wise configuration.



(d) Instantaneous deformed in-line configuration.

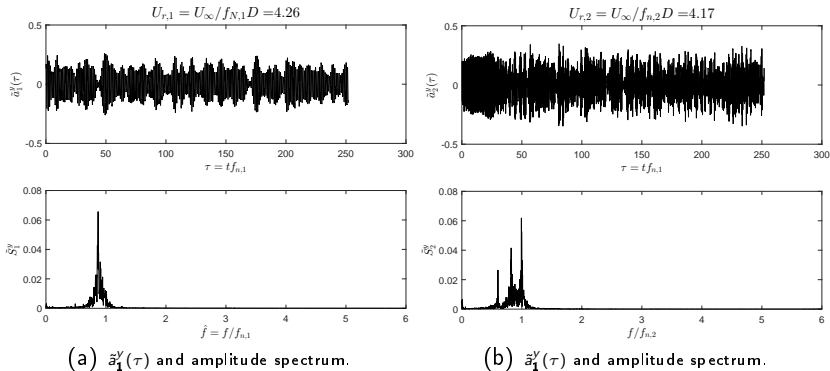


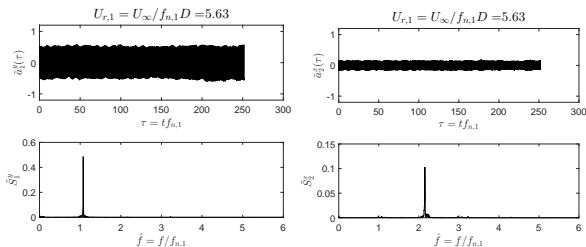
Trajectories on the horizontal plane.



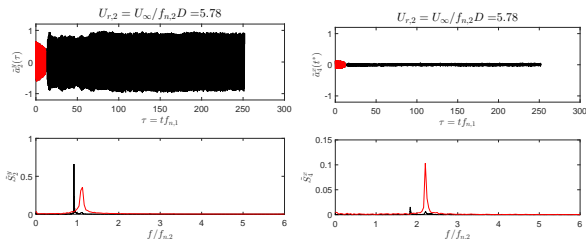
Extracted from Franzini (2019).

- Modal-amplitude time-histories allow investigating the participation of each mode in the response. They contain information of all measured points. We illustrate two modal amplitude time-histories from different tests (different U_∞), but at similar modal reduced velocity $U_{r,k} = U_\infty / f_{n,k} D$. From free-decay tests, $f_{n,2} = 2f_{n,1}$, $f_{n,3} = 3f_{n,1}$



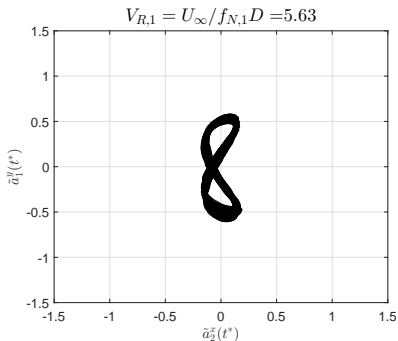


(a) $\tilde{a}_1^y(\tau)$ and amplitude spectrum. (b) $\tilde{a}_2^x(\tau)$ and amplitude spectrum.

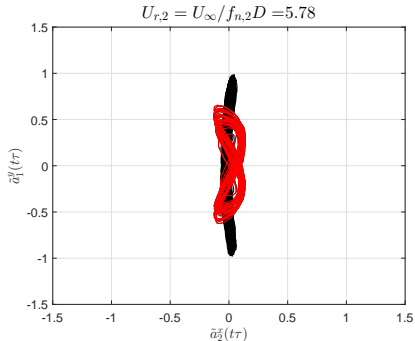


(c) $\tilde{a}_2^y(\tau)$ and amplitude spectrum. (d) $\tilde{a}_4^x(\tau)$ and amplitude spectrum.

$$\tilde{a}_x^{2k} \times \tilde{a}_y^k, U_{r,1} \approx U_{r,2} \approx 5.70.$$

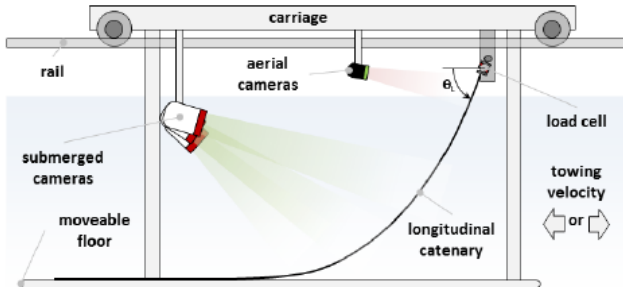


(a) $\tilde{a}_2^x \times \tilde{a}_1^y, U_{r,1} = 5.63.$



(b) $\tilde{a}_4^x \times \tilde{a}_2^y, U_{r,2} = 5.78.$

Extracted from Franzini (2019).



Extracted from Rateiro et al (2016).

- Risers and other slender structures are usually hanged in catenary configuration and their response to VIV are not fully understood;

- Risers and other slender structures are usually hanged in catenary configuration and their response to VIV are not fully understood;
- The angle of incidence between flow and centreline varies along the structure;

- Risers and other slender structures are usually hanged in catenary configuration and their response to VIV are not fully understood;
- The angle of incidence between flow and centreline varies along the structure;
- Use of the independence principle: The flow characteristics are defined only by the component of the free-stream that is normal to the cylinder axis;

- Risers and other slender structures are usually hanged in catenary configuration and their response to VIV are not fully understood;
- The angle of incidence between flow and centreline varies along the structure;
- Use of the independence principle: The flow characteristics are defined only by the component of the free-stream that is normal to the cylinder axis;
- Near or far current incidence plays a role;

- Risers and other slender structures are usually hanged in catenary configuration and their response to VIV are not fully understood;
- The angle of incidence between flow and centreline varies along the structure;
- Use of the independence principle: The flow characteristics are defined only by the component of the free-stream that is normal to the cylinder axis;
- Near or far current incidence plays a role;
- Modal decomposition: Characteristic modal-amplitude *versus* modal reduced velocity exhibit good agreement in different modes.

In the offshore engineering scenario, problems involving VIV occur under combined excitation. Two cases are herein highlighted:

- Concomitant VIV and parametric excitation: Depending on the frequency of the top motion f_t , the response is highly increased (Franzini et al (2016, 2017, 2018)). **Interesting case $f_t : f_{N,1} = 2 : 1$;**

In the offshore engineering scenario, problems involving VIV occur under combined excitation. Two cases are herein highlighted:

- Concomitant VIV and parametric excitation: Depending on the frequency of the top motion f_t , the response is highly increased (Franzini et al (2016, 2017, 2018)). **Interesting case $f_t : f_{N,1} = 2 : 1$;**
- Concomitant VIV and internal flow: The dynamic behavior becomes richer (Meng et al (2017a,2017b)) **Changes in the natural frequencies, decrease in the oscillation amplitudes, mode switching;**

Combined excitation

In the offshore engineering scenario, problems involving VIV occur under combined excitation. Two cases are herein highlighted:

- Concomitant VIV and parametric excitation: Depending on the frequency of the top motion f_t , the response is highly increased (Franzini et al (2016, 2017, 2018)). **Interesting case $f_t : f_{N,1} = 2 : 1$;**
- Concomitant VIV and internal flow: The dynamic behavior becomes richer (Meng et al (2017a,2017b)) **Changes in the natural frequencies, decrease in the oscillation amplitudes, mode switching;**
- Key-point in modeling: *wake-oscillators* are developed and calibrated from “Pure VIV” experiments obtained with rigid and elastically supported cylinders;

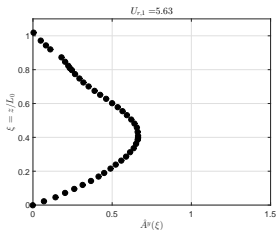
In the offshore engineering scenario, problems involving VIV occur under combined excitation. Two cases are herein highlighted:

- Concomitant VIV and parametric excitation: Depending on the frequency of the top motion f_t , the response is highly increased (Franzini et al (2016, 2017, 2018)). **Interesting case $f_t : f_{N,1} = 2 : 1$;**
- Concomitant VIV and internal flow: The dynamic behavior becomes richer (Meng et al (2017a,2017b)) **Changes in the natural frequencies, decrease in the oscillation amplitudes, mode switching;**
- Key-point in modeling: *wake-oscillators* are developed and calibrated from “Pure VIV” experiments obtained with rigid and elastically supported cylinders;
- Experimental data of VIV under combined excitation are rare. For concomitant VIV and parametric excitation, LMO led a comprehensive experimental campaign that provided these data;

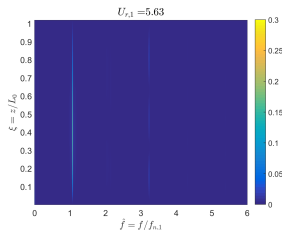
In the offshore engineering scenario, problems involving VIV occur under combined excitation. Two cases are herein highlighted:

- Concomitant VIV and parametric excitation: Depending on the frequency of the top motion f_t , the response is highly increased (Franzini et al (2016, 2017, 2018)). **Interesting case $f_t : f_{N,1} = 2 : 1$;**
- Concomitant VIV and internal flow: The dynamic behavior becomes richer (Meng et al (2017a,2017b)) **Changes in the natural frequencies, decrease in the oscillation amplitudes, mode switching;**
- Key-point in modeling: *wake-oscillators* are developed and calibrated from “Pure VIV” experiments obtained with rigid and elastically supported cylinders;
- Experimental data of VIV under combined excitation are rare. For concomitant VIV and parametric excitation, LMO led a comprehensive experimental campaign that provided these data;
- At least to the best of the author’s knowledge, experimental data concerning concomitant VIV and internal flow excitation are not found.

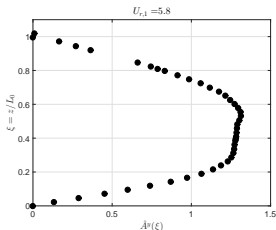
- Combined flexible cylinder VIV and parametric excitation: Experimental results published in Franzini (2018);
- This class focuses on the simultaneous VIV and parametric excitation with $f_t : f_{n,1} = 2 : 1$ and $A_t/L_0 = 1\%$. Figure below, adapted from Franzini (2018), illustrates the cross-wise envelope amplitude and the cross-wise amplitude spectra;
- The simultaneous VIV and parametric excitation with $f_t : f_{n,1} = 2 : 1$ (principal parametric instability in the first mode) significantly affects the response of the hydroelastic system;
- A marked increase in the oscillation amplitude is observed.



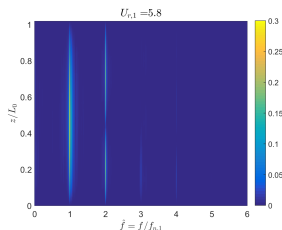
(a) $\hat{A}^y(\xi)$. "Pure VIV".



(b) $S_y(\xi, \hat{f})$. "Pure VIV".



(c) $\hat{A}^y(\xi)$. $f_t : f_{n,1} = 2 : 1$.



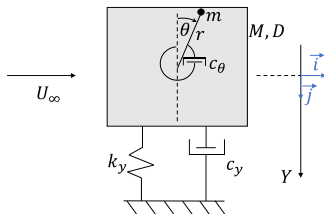
(d) $S_y(\xi, \hat{f})$. $f_t : f_{n,1} = 2 : 1$.

Adapted from Franzini et al (2018).

- Combined flexible cylinder VIV and excitation due to the internal flow is also an important and complex issue → **Ongoing research topic developed at LMO**;
- Usual approach: To consider wake-oscillator models with the same empirically calibrated parameters obtained for rigid and elastically mounted cylinders;
- Superposition of models associated with “pure VIV” and “pure” internal flow excitation;
- Experiments on this combined excitation are quite complex → Planned to be carried out by LMO (part of the PhD research developed by Wagner Defensor).
- In Orsino et al (2018), the numerical results show that there is a range of internal flow velocities associated with VIV mitigation.

Numerical studies

- Focus on the galloping of a square prism, fitted with a rotative NVA;
- Studies developed by Bianca Teixeira (former undergraduate student) and presented in Teixeira et al (2018) and in Franzini (2019).
- Use of the quasi-steady hypothesis;



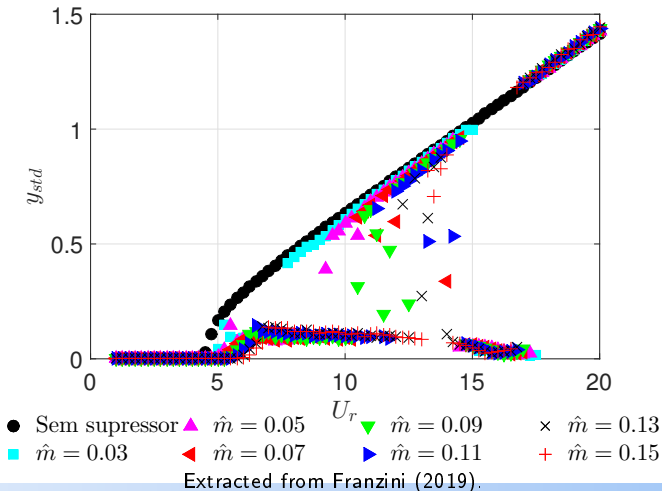
Extracted from Franzini (2019).

- Equations of motion

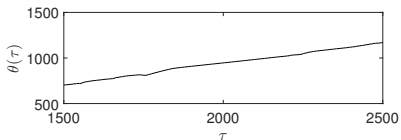
$$(M + m) \frac{d^2 Y}{dt^2} + mr \left[\sin \theta \frac{d^2 \theta}{dt^2} + \cos \theta \left(\frac{d\theta}{dt} \right)^2 \right] + c_y \frac{dY}{dt} + k_y Y = \frac{1}{2} \rho U_\infty^2 DC_y \quad (3)$$

$$mr^2 \frac{d^2 \theta}{dt^2} + mr \sin \theta \frac{d^2 Y}{dt^2} + c_\theta \frac{d\theta}{dt} = 0 \quad (4)$$

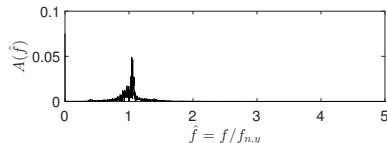
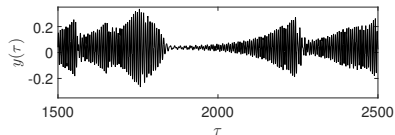
$$\hat{r} = 0.40, \zeta_{\theta} = 0.05, \zeta_y = 0.0009.$$



$$U_r = 12, m = \hat{0}.13, \hat{f} = 0.40, \zeta_\theta = 0.05 \text{ and } \zeta_y = 0.0009.$$



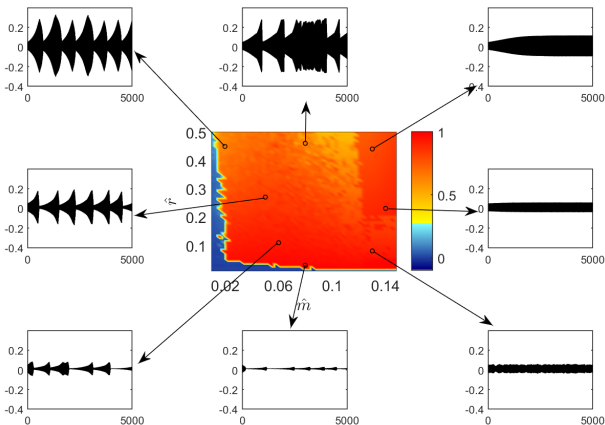
(a) $\theta(\tau)$ and $\cos \theta$.



(b) $y(\tau)$ and amplitude spectrum.

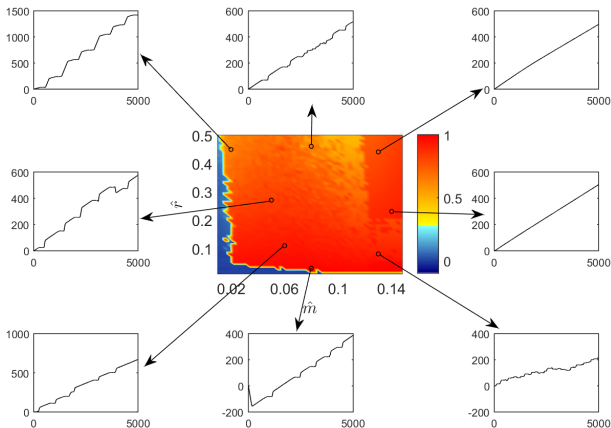
Extracted from Franzini (2019).

$\zeta_\theta = 0.05$ e $U_r = 6.5$. Standard-deviation of the response without suppressor is $y_{std,0} = 0.34$. $\hat{S} = 1 - \frac{y_{std,NVA}}{y_{std,0}}$.



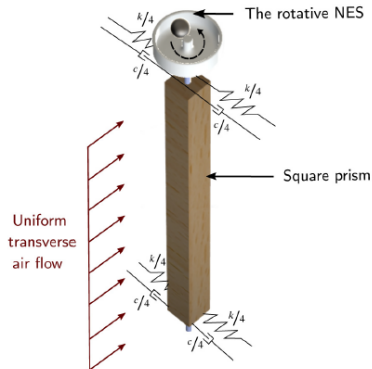
Extracted from Franzini (2019).

$\zeta_\theta = 0.05$ e $U_r = 6.5$. Standard-deviation of the response without suppressor is $y_{std,0} = 0.34$. $\hat{S} = 1 - \frac{y_{std,NVA}}{y_{std,0}}$.



Extracted from Franzini (2019).

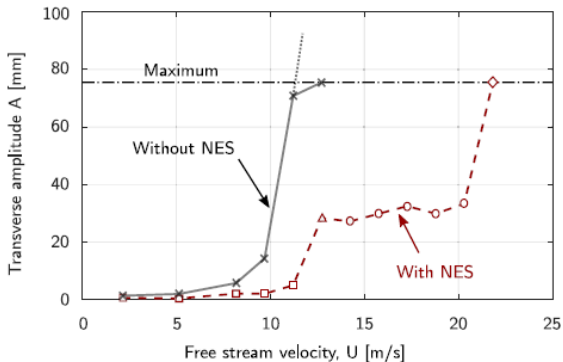
- Wind tunnel experiments carried out at École Polytechnique de Montréal;
- Balls constrained to move along circular tracks;
- Experiments carried out by Michael Selwanis (PhD candidate) and published in Selwanis et al (2021).



Extracted from Selwanis et al (2021).

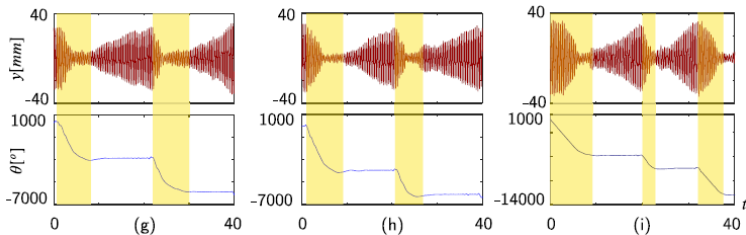
Experimental results

- The proposed suppressor has proved to be highly efficient!



Extracted from Selwanis et al (2021).

- Some features of the response numerically observed appear in the experiments



Extracted from Selwanis et al (2021).

- Vortex-self induced vibrations: VIV associated with oscillatory incoming flow;

- Vortex-self induced vibrations: VIV associated with oscillatory incoming flow;
- Applications in structures hanged in catenary: Motion prescribed to the top of the catenary induces, at each cross-section, oscillatory flow;

- Vortex-self induced vibrations: VIV associated with oscillatory incoming flow;
- Applications in structures hanged in catenary: Motion prescribed to the top of the catenary induces, at each cross-section, oscillatory flow;
- Structural response depends on the amplitude/frequency of the applied motion - see Pesce et al (2017).

- Vortex-self induced vibrations: VIV associated with oscillatory incoming flow;
- Applications in structures hanged in catenary: Motion prescribed to the top of the catenary induces, at each cross-section, oscillatory flow;
- Structural response depends on the amplitude/frequency of the applied motion - see Pesce et al (2017).
- In the dynamics of catenary risers: Motion prescribed to the top+parametric excitation+VIV+internal flow effects=?.

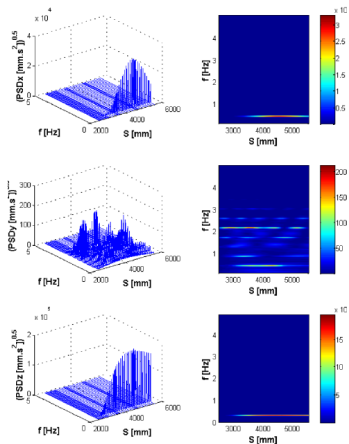


Figure 16. Energy spectra along riser; $2\pi \frac{A_i}{D} = 30$; $f=0.43\text{Hz}$; $f/f_1=1$.

Extracted from Pesce et al (2017).

- Usually, we are interested in mitigating FIV;

- Usually, we are interested in mitigating FIV;
- Recent research topic: energy harvesting - Conversion of part of the mechanical energy available in the vibrating structure into another form of energy (electric energy, for example);

- Usually, we are interested in mitigating FIV;
- Recent research topic: energy harvesting - Conversion of part of the mechanical energy available in the vibrating structure into another form of energy (electric energy, for example);
- Different ways for converting energy: Gravitational potential energy, electromagnetic conversion, piezoelectric conversion;

- Usually, we are interested in mitigating FIV;
- Recent research topic: energy harvesting - Conversion of part of the mechanical energy available in the vibrating structure into another form of energy (electric energy, for example);
- Different ways for converting energy: Gravitational potential energy, electromagnetic conversion, piezoelectric conversion;
- Focus on low-power systems (small sensors, for example).

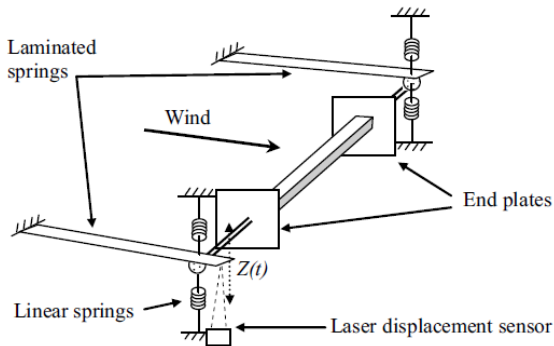
- Tang et al (2009): Flutter of a flexible plate under axial flow and immersed in a magnetic field fitted with wires: Flutter-mill concept;

- Tang et al (2009): Flutter of a flexible plate under axial flow and immersed in a magnetic field fitted with wires: Flutter-mill concept;
- Barrero-Gil et al (2010): Galloping of prismatic bodies → Influence of the cross-section on the energy dissipated at the dashpot;

- Tang et al (2009): Flutter of a flexible plate under axial flow and immersed in a magnetic field fitted with wires: Flutter-mill concept;
- Barrero-Gil et al (2010): Galloping of prismatic bodies → Influence of the cross-section on the energy dissipated at the dashpot;
- Fernandes & Armandei (2014): Torsional galloping is employed for lifting weights;

- Tang et al (2009): Flutter of a flexible plate under axial flow and immersed in a magnetic field fitted with wires: Flutter-mill concept;
- Barrero-Gil et al (2010): Galloping of prismatic bodies → Influence of the cross-section on the energy dissipated at the dashpot;
- Fernandes & Armandei (2014): Torsional galloping is employed for lifting weights;
- Franzini et al (2016,2017): Concomitant parametric excitation and galloping increases the harvested power in piezoelectric circuits.

Magnets are placed at the tip of the leaves-springs and can move relative to coils.



Extracted from Hémon et al (2017).

- Bernitsas et al (2006): VIVACE (Vortex-Induced Vibrations Aquatic Clean Energy) project → Experimental device based on VIV of a series of aligned (tandem) cylinders. **Electromagnetic effect**;

Energy harvesting from VIV

- Bernitsas et al (2006): VIVACE (Vortex-Induced Vibrations Aquatic Clean Energy) project → Experimental device based on VIV of a series of aligned (tandem) cylinders. **Electromagnetic effect**;
- Grouthier et al (2012,2014): Energy harvesting from VIV → wake-oscillator models (VIV-1dof) and energy is harvested at the dashpot;

Energy harvesting from VIV

- Bernitsas et al (2006): VIVACE (Vortex-Induced Vibrations Aquatic Clean Energy) project → Experimental device based on VIV of a series of aligned (tandem) cylinders. **Electromagnetic effect**;
- Grouthier et al (2012,2014): Energy harvesting from VIV → wake-oscillator models (VIV-1dof) and energy is harvested at the dashpot;
- Mehmood et al (2013): Rigid cylinders, mounted on piezoelectric supports → Electric power is harvested from the electrical resistance. CFD is employed for modeling the hydrodynamic load;

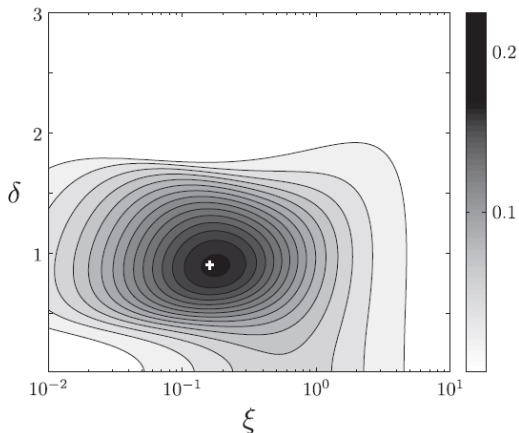
Energy harvesting from VIV

- Bernitsas et al (2006): VIVACE (Vortex-Induced Vibrations Aquatic Clean Energy) project → Experimental device based on VIV of a series of aligned (tandem) cylinders. **Electromagnetic effect**;
- Grouthier et al (2012,2014): Energy harvesting from VIV → wake-oscillator models (VIV-1dof) and energy is harvested at the dashpot;
- Mehmood et al (2013): Rigid cylinders, mounted on piezoelectric supports → Electric power is harvested from the electrical resistance. CFD is employed for modeling the hydrodynamic load;
- Bunzel & Franzini (2017), Franzini & Bunzel (2018): Piezoelectric energy harvesting from VIV → Pioneer in including in-line oscillations in the analysis. Sensitivity studies focusing on the influence of the piezoelectric parameters;

Energy harvesting from VIV

- Bernitsas et al (2006): VIVACE (Vortex-Induced Vibrations Aquatic Clean Energy) project → Experimental device based on VIV of a series of aligned (tandem) cylinders. **Electromagnetic effect**;
- Grouthier et al (2012,2014): Energy harvesting from VIV → wake-oscillator models (VIV-1dof) and energy is harvested at the dashpot;
- Mehmood et al (2013): Rigid cylinders, mounted on piezoelectric supports → Electric power is harvested from the electrical resistance. CFD is employed for modeling the hydrodynamic load;
- Bunzel & Franzini (2017), Franzini & Bunzel (2018): Piezoelectric energy harvesting from VIV → Pioneer in including in-line oscillations in the analysis. Sensitivity studies focusing on the influence of the piezoelectric parameters;
- Madi et al (2019): Developed by Leticia Madi (PhD candidate), this paper deals with piezoelectric energy harvesting from flexible cylinder VIV.

Existence of a critical structural damping ratio ξ for maximizing energy harvesting efficiency.



Extracted from Grouthier et al (2014).

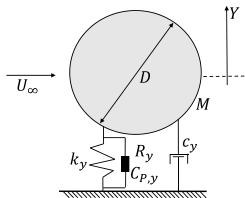
Piezoelectric energy harvesting from VIV

- The rigid cylinder is assembled onto a piezoelectric support. The electrical circuit is characterized by its capacitance $C_{P,y}$ and resistance R_y . θ_y is the electromechanical coupling term.
- For the VIV-1dof condition, the solid-fluid-electric system is governed by:

$$(M + m_a^{pot}) \frac{d^2 Y}{dt^2} + c_y \frac{dY}{dt} + k_y Y - \theta_y V_y = \frac{1}{2} \rho U_\infty^2 DLC_{y,v} \quad (5)$$

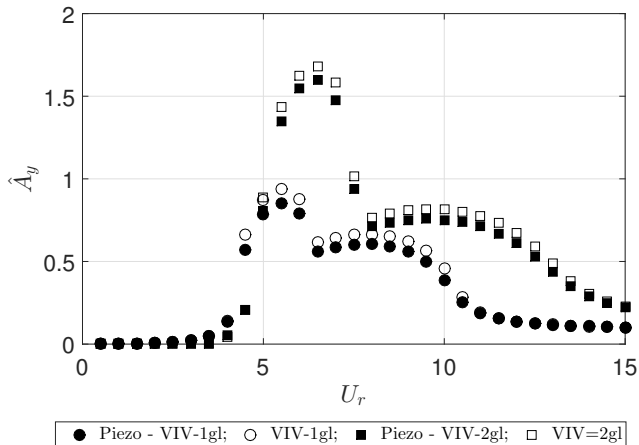
$$\frac{d^2 q_y}{dt^2} + \epsilon_y \omega_f (q_y^2 - 1) \frac{dq_y}{dt} + \omega_f^2 q_y = \frac{A_y}{D} \frac{d^2 Y}{dt^2} \quad (6)$$

$$C_{P,y} \frac{dV_y}{dt} + \frac{V_y}{R_y} + \theta_y \frac{dY}{dt} = 0 \quad (7)$$



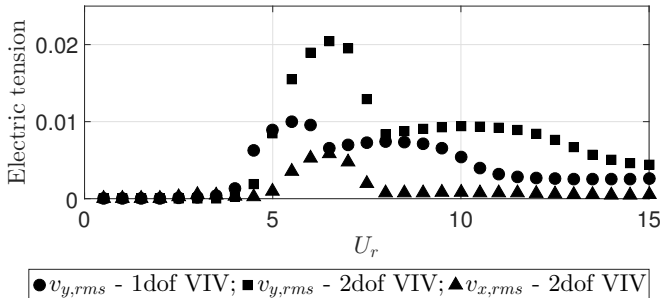
Extracted from Franzini & Bunzel (2018).

- Due to energy harvesting, a small decrease in the cylinder response.



Adapted from Franzini & Bunzel (2018).

- Energy harvesting is more efficient if the cylinder is assembled onto a 2dof elastic support.



Extracted from Franzini & Bunzel (2018).